Eur. Phys. J. C 5, 317–326 (1998)
DOI 10.1007/s100529800844

THE EUROPEAN PHYSICAL JOURNAL C

Single pseudoscalar meson production in diffractive ep scattering*

W. Kilian, O. Nachtmann

Institut für Theoretische Physik, Universität Heidelberg, Philosophenweg 16, D-69120 Heidelberg, Germany
(e-mail: W.Kilian@thphys.uni-heidelberg.de, O.Nachtmann@thphys.uni-heidelberg.de)

Received: 18 December 1997 / Published online: 10 March 1998

Abstract. Exclusive pseudoscalar meson production in ep scattering at high energies is a direct probe for a possible "odderon" exchange in soft hadronic processes. Using a simple phenomenological ansatz for the odderon, we demonstrate how it can be separated from the contribution due to photon-photon fusion, and the relevant parameters be measured. Total cross sections and differential distributions are presented for π^0, η, η', and η_c production. Results are given from both a full calculation and one using the equivalent photon approximation. The accuracy of the latter is discussed.

1 Introduction

Although QCD is well established as the theoretical framework of hadronic phenomena, it has remained a great challenge to derive results for *soft* hadronic interactions from first principles, *i.e.*, starting from the Lagrangian of QCD. In particular, one would like to understand high-energy diffractive reactions. Pioneering work in this direction using perturbation theory can be found in [1–4]. A more general framework was developed in [5–8], where both nonperturbative and perturbative effects can be treated. In this way, a description of high-energy diffractive reactions in terms of the vacuum parameters of QCD and of hadron extension parameters was achieved, which gives very satisfactory agreement with experimental results [7].

On the other hand, high-energy reactions can be described by a Regge-pole model (for reviews, cf. [9]). Its application to diffractive reactions is very successful ([10], cf. also [11]). For simplicity, in this paper we will use Regge-pole parameterizations for the hadronic amplitudes occurring in our calculations.

Consider, for instance, elastic scattering of two hadrons $h_{1,2}$

$$h_1(p_1) + h_2(p_2) \to h_1(p_3) + h_2(p_4), \tag{1}$$

and let s, t, u be the usual Mandelstam variables

$$s = (p_1 + p_2)^2, \qquad t = (p_1 - p_3)^2, \qquad u = (p_1 - p_4)^2. \tag{2}$$

The Regge-pole ansatz for the T-matrix element of reaction (1) reads as follows:

$$T(s,t,u) = \sum_i c_i(t)\,(s/s_0)^{\alpha_i(t)-1}. \tag{3}$$

Here the individual terms correspond to the Regge poles which can be exchanged in the reaction (1), and $\alpha_i(t)$ are their trajectories which turn out to be linear to a good approximation:

$$\alpha_i(t) = \alpha_i(0) + \alpha_i' t. \tag{4}$$

While the parameters $\alpha_i(0)$ and α_i' which govern the s and part of the t dependence are observed to be universal, the coupling parameters c_i containing the spin and signature factors and Regge residues depend on the hadrons participating in the particular process considered. The scale factor needed for dimensional reasons is denoted by s_0. Each Regge pole is associated with a family of hadrons exchanged [9,12].

The Regge pole corresponding to the leading term in (3) for $s \to \infty$ is called the *pomeron*. Typical values for its parameters are [10]

$$\alpha_{\mathbb{P}}(0) = 1.08, \qquad \alpha_{\mathbb{P}}' = 0.25\ \mathrm{GeV}^{-2}. \tag{5}$$

The pomeron has vacuum quantum numbers, in particular charge conjugation $C = +1$. The simplest description of such an interaction in perturbative QCD is by two-gluon exchange [1]. Thus, one expects the pomeron to be associated to a family of glueball states, the lowest-lying one of these having quantum numbers $J^{PC} = 2^{++}$. Lattice calculations [13] support a mass for this state around 2 GeV which would fit nicely onto the pomeron trajectory [14]. The experimental situation concerning 2^{++} glueball states is summarized in [11]. Detailed theoretical investigations of the pomeron in perturbative QCD can be found in [15, 16].

A natural question is whether there exist effects in high-energy hadron-hadron scattering where the s-dependence is similar to the one induced by the pomeron, but

* Work supported by German Bundesministerium für Bildung und Forschung (BMBF), Contract Nr. 05 6HD 91 P(0)

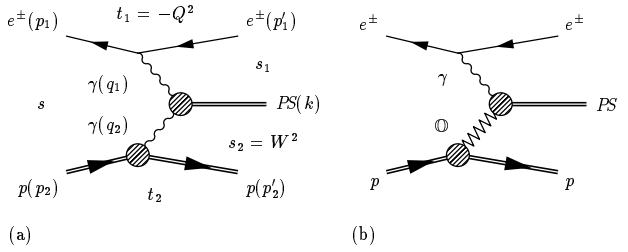

Fig. 1. Feynman diagrams for pseudoscalar meson production in *ep* scattering at high energies with photon **a** and odderon **b** exchange

which are connected with $C = -1$ exchange. In the framework of the Regge-pole model, the corresponding object has been called the *odderon* [17–20]. Various possibilities were discussed for it, ranging from a moving pole, similar to the pomeron case, to exotic possibilities such as two complex poles [18]. In perturbative QCD, an odderon arises in diagrams where three or more gluons are exchanged. Indeed, both in perturbative [21–24] and in nonperturbative [6,25] calculations one finds no reason for the odderon contribution to be particularly small in quark-quark scattering. [However, since free quarks do not exist, this process cannot be studied by itself in experiments.] On the other hand, no odderon has so far been observed in hadron-hadron elastic scattering (1) for $s \to \infty$, $|t|$ small. Possible resolution of this puzzle have been proposed in [26,27].

Thus, experimental searches for the odderon are clearly worthwhile. Evidence for either the presence or absence of such effects will give important clues on the structure of diffractive interactions in QCD.

In [28] it has been pointed out that exclusive pseudoscalar meson production in $e^\pm p$ collisions at high energies (for HERA: $\sqrt{s} = 300.6$ GeV) is a direct probe for the odderon (Fig. 1):

$$e^\pm p \to e^\pm p\, PS, \tag{6}$$

where *PS* generically denotes a meson with the quantum numbers $J^{PC} = 0^{-+}$, in particular, $PS = \pi^0, \eta, \eta'$, or η_c. Since the quantum numbers exchanged in the hadronic interaction (Fig. 1b) are those of the photon, the process (6) can proceed also via photon-photon fusion (Fig. 1a). Here and in the following we always work in leading-order perturbation theory of the electroweak interactions. Adopting standard parameterizations for the proton and meson form factors, the diagram in Fig. 1a can easily be calculated. Note that the exchange of an object with vacuum quantum numbers, *i.e.*, of the pomeron, is forbidden in reaction (6).

In the present paper we will extend the considerations in [28] and study, from a purely phenomenological point of view, the effect of an odderon interaction on the process (6) and the possibilities to extract detailed information about its properties.

The kinematical variables are as indicated in Fig. 1a. In addition, in accordance with the usual notation for deep-inelastic scattering processes, we introduce the fractional energy loss of the electron

$$y = \frac{p_2 \cdot (p_1 - p_1')}{p_2 \cdot p_1}, \tag{7}$$

where $0 \le y \le 1$.

If the outgoing proton is not observed, the signal consists of the outgoing electron and of the decay products of the *PS* particle, *e.g.*, a $\gamma\gamma$ pair. The numbers and distributions presented in the following sections refer either to the complete phase space or to two particular sets of cuts appropriate for the HERA environment [29] defined and denoted as follows:

$$0.3 < y < 0.7, \quad 0 < Q^2 < 0.01\ \text{GeV}^2, \quad \textit{Photoproduction (PP)}, \tag{8}$$

$$0.3 < y < 0.7, \quad 1\ \text{GeV}^2 < Q^2, \quad \textit{Deep inelastic scattering (DIS)}, \tag{9}$$

where $Q^2 \equiv -q_1^2$.

2 Meson form factor parameterization

The coupling of a pseudoscalar meson $PS = \pi^0, \eta, \eta', \eta_c$ to two photons has the form

$$iu\epsilon_{\mu\nu\rho\sigma} q_1^\rho q_2^\sigma\, T(q_1^2, q_2^2), \tag{10}$$

where, by definition, $T(0,0) = 1$. The dimensionful coupling constant u is related to the triangle anomaly. In terms of the meson decay constant f_{PS}, it is given by

$$u = \alpha/(\pi f_{PS}). \tag{11}$$

We choose a convention where $f_\pi = 93$ MeV, $\alpha \equiv e^2/4\pi$ is the fine-structure constant, and e the proton charge. From (10,11) we find for the partial width $\Gamma_{\gamma\gamma}$ for $PS \to \gamma\gamma$:

$$\Gamma_{\gamma\gamma} = \frac{u^2}{64\pi} m_{PS}^3 \tag{12}$$

For our numerical results we use thus

$$u = \sqrt{64\pi\Gamma_{\gamma\gamma}/m_{PS}^3}, \tag{13}$$

with $\Gamma_{\gamma\gamma}$ taken from experiment (cf. Table 1).

The form factor $T(q_1^2, q_2^2)$ is known as the *transition form factor* of the pseudoscalar meson. It can be measured in pseudoscalar production in e^+e^- scattering, $e^+e^- \to e^+e^- PS$. The diagram for this reaction is as in Fig. 1a, but with the proton replaced by an electron line. It is found that the formula

$$T(q_1^2, 0) = \frac{1}{1 - q_1^2/8\pi^2 f_{PS}^2} \tag{14}$$

introduced by Brodsky and Lepage [30], which is confirmed by constituent quark model [31] and QCD sum-rule calculations [32], fits the data for $q_1^2 \neq 0$, $q_2^2 = 0$

Table 1. Pseudoscalar meson data, from [11]

	π^0	η	η'	η_c
m [MeV]	134.9764(5)	547.45(19)	957.77(14)	2979.8(2.1)
$\Gamma_{\rm tot}$ [MeV]	$7.8(6)\times10^{-6}$	$1.18(11)\times10^{-3}$	0.201(16)	13.2(3.8)
BR($\gamma\gamma$) [%]	98.798(32)	39.25(31)	2.12(13)	0.30(12)
u [GeV^{-1}]	0.025(1)	0.024(1)	0.031(1)	0.0075(15)

reasonably well [33]. Within the experimental errors, the formula (14) coincides in this kinematic region with the double pole form suggested by vector meson dominance

$$T(q_1^2,q_2^2)=\frac{1}{(1-q_1^2/\Lambda^2)(1-q_2^2/\Lambda^2)}, \tag{15}$$

where for the light mesons, Λ is given by the ρ (or ω) meson mass. For η_c production, one expects a slower decrease of the form factor with q_i^2 [34]; one should then insert the J/ψ mass for Λ in (15).

Precise data are available only for $T(q^2,0)$, *i.e.*, with one photon nearly on-shell. For both photons far off-shell, perturbative QCD predicts [35]

$$T(q_1^2,q_2^2)=-\frac{8\pi^2}{3}f_{PS}^2\int_0^1 dx\frac{\varphi(x,\bar x)}{xq_1^2+\bar x q_2^2}, \tag{16}$$

with $\bar x\equiv 1-x$. The amplitude $\varphi(x,\bar x)$ is normalized ($\int dx\,\varphi(x,\bar x)=1$) and has the asymptotic form

$$\varphi(x,\bar x)=6x\bar x. \tag{17}$$

The form (15) is not compatible with (16). One might worry whether this discrepancy has an impact on the quantitative predictions for pseudoscalar meson productions that will be presented below. For comparison, we introduce a formula which interpolates between the asymptotic limit (16) and the on-shell limit $T=1$ for both q^2 nonvanishing:

$$\begin{aligned}T(q_1^2,q_2^2)&=-\frac{8\pi^2}{3}f_{PS}^2\int_0^1 dx\frac{\varphi(x,\bar x)}{xq_1^2+\bar x q_2^2-8\pi^2f_{PS}^2/3}\\&=8\pi^2f_{PS}^2\left(-\frac{\hat q_1^2+\hat q_2^2}{(\hat q_1^2-\hat q_2^2)^2}+\frac{2\hat q_1^2\hat q_2^2}{(\hat q_1^2-\hat q_2^2)^3}\ln\frac{\hat q_1^2}{\hat q_2^2}\right),\end{aligned} \tag{18}$$

where $\hat q_i^2\equiv q_i^2-8\pi^2f_{PS}^2/3$. This form agrees with (14) for $q_1^2\neq0$, $q_2^2=0$, and with (16) for $q_{1,2}^2\neq0$, up to corrections which scale like $\log|q_i^2|/q_i^4$ in the limit $q_i^2\to-\infty$. In Fig. 2 we compare the shape of the above form factor expressions for two fixed values of q_2^2. At $q_2^2=0$ all three curves are close to each other. By contrast, at $q_2^2=4$ GeV^2, the interpolation curve (18) lies considerably higher than the naive double pole ansatz (15), which we use as standard parameterization in the following. However, we find that if the alternative form factor (18) is inserted, the shift in the cross section values and distributions discussed below is numerically below 1% in all cases.

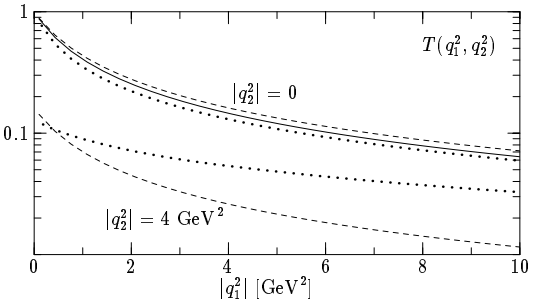

Fig. 2. Various parameterizations for the pion transition form factor $T(q_1^2,q_2^2)$. The *solid curve* represents the Brodsky-Lepage formula (14). The *dashed* and *dotted* curves correspond to the double pole form (15) and the interpolation formula (18), respectively

3 Results for the two-photon process

Once the form factors are given, the photon-photon amplitude (Fig. 1a) is determined completely. The spin-averaged squared matrix element has the form [36]

$$\frac14|M|^2=2\Delta\frac{u^2|T(t_1,t_2)|^2}{t_1t_2}\rho_e^{++}\rho_p^{++}, \tag{19}$$

where

$$\Delta=\frac14(m_{PS}^2-t_1-t_2)^2-t_1t_2 \tag{20}$$

is the phase space function for the subprocess $\gamma^*\gamma^*\to PS$. We have assumed that the azimuthal angles of the outgoing particles are not observed. The probabilities for photon emission off the initial electron/positron and proton, are given by ρ_e^{++} and ρ_p^{++}, respectively, with

$$\rho_e^{++}=1+2\frac{m_e^2}{q_1^2}+\frac{1}{2\Delta}\left[4(p_1q_2)(p_1'q_2)+q_1^2q_2^2\right] \tag{21}$$

$$\begin{aligned}\rho_p^{++}&=C(t_2)+D(t_2)\\&\quad\times\left(2\frac{m_p^2}{q_2^2}+\frac{1}{2\Delta}\left[4(p_2q_1)(p_2'q_1)+q_1^2q_2^2\right]\right)\end{aligned} \tag{22}$$

The coefficient functions C and D are determined by the electric and magnetic form factors of the proton:

$$C(t_2)=G_M^2(t_2),\qquad D(t_2)=\frac{4m_p^2G_E^2(t_2)-t_2G_M^2(t_2)}{4m_p^2-t_2} \tag{23}$$

We use the standard dipole parameterization

$$G_E(t) = \frac{1}{(1 - t/m_D^2)^2}, \qquad G_M(t) = \mu_p\, G_E(t), \tag{24}$$

with $m_D^2 = 0.71\ \mathrm{GeV}^2$ and $\mu_p = 2.7928$ [37].

Finally, we note that longitudinal photon polarizations do not contribute in (19) due to the coupling (10).

For the calculation of two-photon processes, equivalent-photon approximations (EPA) are commonly used. Therefore, in the following sections we compare two different versions of the EPA with a numerical integration of the exact expression for the cross section, and discuss the accuracy of the approximations in various kinematical regions.

3.1 Double Equivalent Photon Approximation (DEPA)

Since the dominant contribution to the $\gamma\gamma$-fusion process arises from the region in phase space where both photon virtualities are small, *i.e.*, $|t_1|, |t_2| \ll m_{PS}^2, m_\rho^2$, an estimate for the total cross section may be found from the DEPA [36]. Introducing the fractional energy losses

$$x_i = \frac{E_i - E_i'}{E_i}, \qquad \bar{x}_i \equiv 1 - x_i \tag{25}$$

of the incoming $e^\pm$ ($i = 1$) and proton ($i = 2$), the total cross section is given by

$$\sigma(ep \to ep + PS) = \int_0^1 \frac{dx_1}{x_1}\frac{dx_2}{x_2}\, n_1(x_1)\, n_2(x_2) \times \frac{\pi u^2 m_{PS}^2}{8s}\delta(x_1 x_2 - m_{PS}^2/s) \tag{26}$$

with the photon fluxes

$$n_i(x) = \frac{\alpha}{\pi}\left[\left(1 - x + \mu_i^2\frac{x^2}{2}\right)\ln\frac{t_{i,\min}}{t_{i,\max}} - (1-x)\left(1 - \frac{t_{i,\min}}{t_{i,\max}}\right)\right], \tag{27}$$

where μ_i is the magnetic moment of the incoming $e^\pm$ resp. proton. The photon virtualities t_i have been integrated over the range

$$t_{i,\min} \equiv -\Lambda^2 = -\min(m_{PS}^2, m_\rho^2, q_0^2),$$
$$t_{i,\max} = -\frac{x_i^2}{1 - x_i} m_i^2. \tag{28}$$

where $m_{1,2}$ is given by m_e and m_p, respectively. Within the validity of the DEPA, it is legitimate to replace the detailed t_i dependence of the meson and proton form factors by an appropriate sharp cutoff Λ^2.

The delta function in (26) restricts the integration range for the independent x variable between $((m_p + m_{PS})^2 - m_p^2)/s$ and 1. The error of the approximation is of the order

$$\Delta\sigma/\sigma \sim \frac{1}{\ln|t_{\max}|/\Lambda^2}. \tag{29}$$

which depends on x_1 and x_2.

Within the validity range of the DEPA, the following simplifications apply (cf. Fig. 1):

$$y = x_1, \qquad W^2 = ys, \qquad s_1 = \frac{m_{PS}^2}{y}, \qquad Q^2 = 0. \tag{30}$$

Furthermore, the rapidity of the produced pseudoscalar has the value

$$\eta = \eta_{\mathrm{cm}} - \frac{1}{2}\log\frac{x_1}{x_2} = \eta_{\mathrm{cm}} - \log\frac{\sqrt{s}}{m_{PS}} - \log y, \tag{31}$$

where η_{cm} is the rapidity of the c.m. system of the incoming particles. [At HERA, $\eta_{\mathrm{cm}} = 1.69$, where we choose the usual convention that the initial proton momentum points in positive z-direction.]

3.2 Single Equivalent Photon Approximation (EPA)

This approximation can be used in the photoproduction region where $-t_1 = Q^2 < 0.01\ \mathrm{GeV}^2$ is small, but $|t_2|$ can become large. Then the DEPA is no longer applicable. However, the photon $\gamma(q_1)$ emitted by the initial electron/positron is still essentially on-shell and may be treated within the EPA. The corresponding approximation to the total cross section reads

$$\sigma(s) = \int_{y_{\min}}^{y\max}\frac{dy}{y}n(y)\int_{t_{\min}}^{t\max} dt_2\,\frac{d\hat{\sigma}}{dt_2} \qquad \text{with}$$
$$s_2 = ys + (1-y)m_p^2, \tag{32}$$

where

$$\frac{d\hat{\sigma}}{dt_2} = \frac{e^2u^2|T(t_2,0)|^2}{64\pi(s_2 - m_p^2)^2 t_2} \times\big\{|F_1(t_2)|^2\big[-2t_2^{-1}m_p^2 m_{PS}^4 - 2m_p^4 + 2m_p^2 m_{PS}^2 - m_{PS}^4 + 4m_p^2 s_2 + 2m_{PS}^2 s_2 - 2s_2^2 + t_2(2m_{PS}^2 - 2s_2) - t_2^2\big] + \frac{1}{2m_p^2}|F_2(t_2)|^2\big[-m_p^2 m_{PS}^4 + t_2(m_p^4 + 3m_p^2 m_{PS}^2 - 2m_p^2 s_2 - m_{PS}^2 s_2 + s_2^2) + t_2^2(-2m_p^2 + s_2)\big]\big\}. \tag{33}$$

Here $F_{1,2}(t_2)$ are the Dirac and Pauli form factors, which are related to G_E, G_M by

$$G_E(t_2) \equiv F_1(t_2) + t_2\frac{1}{4m_p^2}F_2(t_2)\,,$$
$$G_M(t_2) \equiv F_1(t_2) + F_2(t_2)\,. \tag{34}$$

The kinematic limits for the integrations in (32) are given by

$$y_{\min} = \frac{(2m_p + m_{PS})m_{PS}}{s - m_p^2}, \qquad y_{\max} = 1, \tag{35}$$

and

$$t_{\min,\,\max} = \frac{m_{PS}^4}{4s_2} - \left[\frac{s_2 - m_p^2}{2\sqrt{s_2}} \pm \sqrt{\frac{(s_2 + m_{PS}^2 - m_p^2)^2}{4s_2} - m_{PS}^2}\right]^2 . \quad (36)$$

The above formulae can easily be implemented in a Monte Carlo event generator, which we have used to generate the distributions in the PP region in the following sections. The error of the approximation depends on y; for y values of order unity, it is usually estimated as [36]

$$\Delta\sigma/\sigma \sim \frac{Q^2_{\max}}{\Lambda^2}\,\frac{1}{\ln Q^2_{\max}/m_e^2}, \quad (37)$$

where $Q^2_{\max} = 0.01\ \mathrm{GeV}^2$ for the PP cuts (8), and Λ is the effective cutoff which enters the *PS* form factor.

3.3 Full calculation

In order to have a reliable result in all regions of phase space, an exact integration of the squared matrix element (19) is necessary. This is nontrivial in practice since at the edge of phase space large cancellations occurr in (19). To obtain numerically stable results, we used the `CompHEP` [38] kinematical module with quadruple precision numerics for the integration and event generation[1].

In Table 2 we display the total cross sections for π^0, η, η', and η_c production at HERA as well as the cross sections in the PP and DIS regions, using the three methods of calculation introduced above. Note that there is an overall error in the cross sections coming from the experimental uncertainty in the mesonic $\gamma\gamma$ width (cf. Table 1) which amounts to 10% for π^0, η, and η', and is as large as 50% for the η_c meson.

Whereas the DEPA is an approximation at the 20% level, the EPA gives quite accurate results, in particular in the PP region. It is interesting, however, that for π^0 photoproduction the standard formula (37) underestimates the actual error of the EPA by more than a factor 10. This is due to the fact that the photon-proton scattering amplitude is singular at $t_2 = 0$, which introduces a logarithmic dependence on the lower kinematical limit of $|t_2|$. For large s_2 this limit simplifies to

$$t_{\max} \approx -\frac{m_p^2(m_\pi^2 + Q^2)^2}{s_2^2}. \quad (38)$$

The EPA neglects the nonzero value of Q^2. As a result, the EPA estimate has an additional error of magnitude

$$\Delta\sigma/\sigma \sim \frac{Q^2_{\max}}{m_\pi^2}\,\frac{1}{\ln s/m_\pi^2} \approx 5\%. \quad (39)$$

[1] Recently, a Monte Carlo generator which includes the full kinematical dependence has been developed for the analogous $\gamma\gamma$ processes in e^+e^- collisions [39]

Table 2. Total cross sections in pb for pseudoscalar meson production at HERA. The kinematical regions are defined in (8) and (9), and the calculational methods are described in the text. The statistical errors of the Monte Carlo integration are at the permille level

		π^0	η	η'	η_c
tot	DEPA	1500	1200	1700	65
	EPA	1803	1011	1320	51.0
	full	1801	983	1276	50.3
PP	DEPA	84	62	93	4.2
	EPA	78.1	56.4	83.6	3.83
	full	74.7	56.3	83.5	3.84
DIS	full	0.46	0.41	0.65	0.49

In the DIS region neither the DEPA nor the EPA are reliable, and we just quote the result from the full calculation.

4 Odderon exchange

Introducing now a possible odderon exchange contribution to (6) (cf. Fig. 1b), we make an ansatz similar to the one made in [10] for the pomeron. Thus, we assume the effective odderon "propagator" (Fig. 3) to be given by

$$(-i)\eta_{\mathbb{O}}\,(-is/s_0)^{\alpha_{\mathbb{O}}(t)-1} g^{\mu\nu} \quad (40)$$

where $\alpha_{\mathbb{O}}(t)$ is the odderon trajectory which we assume to be linear

$$\alpha_{\mathbb{O}}(t) = \alpha_{\mathbb{O}}(0) + \alpha'_{\mathbb{O}} t \quad (41)$$

In (40), $\eta_{\mathbb{O}} = \pm 1$ determines the phase of the odderon amplitudes, which is not known *a priori*. The odderon couplings are given as follows:

For the quark-odderon coupling (Fig. 3b) we set

$$-i\beta_{\mathbb{O}}\gamma^\lambda \quad (42)$$

and for the proton-odderon coupling (Fig. 3c)

$$-i\,3\beta_{\mathbb{O}}\left[F_1^{(0)}(q^2)\,\gamma^\lambda + \frac{i}{2m_p}F_2^{(0)}(q^2)\,\sigma^{\lambda\nu}q_\nu\right] \quad \text{with } q = p' - p. \quad (43)$$

Here

$$F_i^{(0)}(q^2) = F_i^p(q^2) + F_i^n(q^2), \qquad i = 1, 2 \quad (44)$$

are the isoscalar nucleon form factors, and $\beta_{\mathbb{O}}$ is the analogue of the quark-pomeron coupling constant $\beta_{\mathbb{P}}$ of [10].

In the following we will neglect the neutron form factors in (44) and set $F_i^{(0)}(q^2) = F_i^p(q^2)$ for simplicity. This is a good approximation for the Dirac form factor $F_1^{(0)}(q^2)$ since $|F_1^n(q^2)| \ll |F_1^p(q^2)|$, and the contribution of the

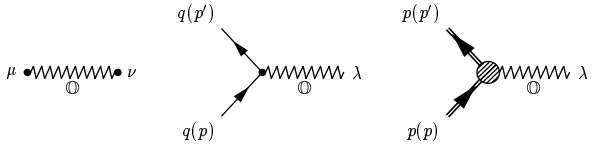

Fig. 3. Diagrammatic representations of the odderon propagator (40) and its couplings to quarks (42) and protons (43)

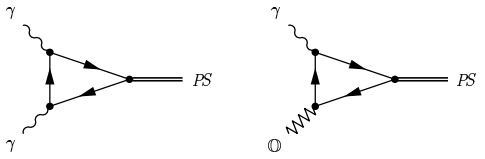

Fig. 4. Diagrams for the $\gamma\gamma PS$ and $\gamma\mathbb{O}PS$ form factors. The *crossed diagrams* are to be added

Pauli form factor $F_2^{(0)}(q^2)$ is small in the region of small $|q^2|$ where most of the cross section in the processes considered here comes from.

The difference of the ratios ρ of the real and imaginary parts of the forward $\bar{p}p$ and pp scattering amplitudes is then given by

$$\rho^{\bar{p}p}(s)-\rho^{pp}(s)=-2\eta_{\mathbb{O}}\left(\frac{\beta_{\mathbb{O}}}{\beta_{\mathbb{P}}}\right)^2\left(\frac{s}{s_0}\right)^{\alpha_{\mathbb{O}}(0)-\alpha_{\mathbb{P}}(0)} \times\frac{\cos\left[\frac{\pi}{2}(\alpha_{\mathbb{O}}(0)-1)\right]}{\cos\left[\frac{\pi}{2}(\alpha_{\mathbb{P}}(0)-1)\right]} \times\left[1+\mathcal{O}(\beta_{\mathbb{O}}^2/\beta_{\mathbb{P}}^2,\,\alpha_{\mathbb{P}}(0)-1)\right]. \quad (45)$$

where we assume the model of [10] for pomeron exchange.

At energies $\sqrt{s}\gtrsim 100$ GeV where non-leading Regge pole contributions should be negligible, we have results only for $\rho^{\bar{p}p}$ from $\bar{p}p$ collision experiments [40]. One has to resort to dispersion theory calculations (cf., *e.g.*, [20]) to extract ρ^{pp} from data. We take as an estimate

$$|\rho^{\bar{p}p}(s)-\rho^{pp}(s)|\lesssim 0.05 \qquad \text{for } \sqrt{s}>100\text{ GeV}. \quad (46)$$

To translate this into information on the ratio $\beta_{\mathbb{O}}/\beta_{\mathbb{P}}$ we still need to know the value of $\alpha_{\mathbb{O}}(0)-\alpha_{\mathbb{P}}(0)$ in (45). Assuming, for instance, $\alpha_{\mathbb{O}}(0)=1$, which is suggested by the field-theoretic arguments of [6] and the results of [22], we get

$$(\beta_{\mathbb{O}}/\beta_{\mathbb{P}})^2\lesssim 0.05. \quad (47)$$

Certainly, we do *not* claim this to be a bound on odderon contributions in pp and $\bar{p}p$ scattering. But (47) should give an idea on the strength of a possible odderon in conventional Regge parameterizations.

Considering the ratio of the odderon and photon couplings to the produced meson, one naturally expects that the $\gamma\gamma$ coupling is proportional to the electromagnetic charge squared of the quark states within the meson, whereas for the $\gamma\mathbb{O}$ coupling only a single charge factor enters, if the odderon is assumed to be flavor-blind. Thus, for a meson of quark content

$$PS\sim\sum_i a_{PS}^i\, q_i\bar{q}_i, \quad (48)$$

in a valence quark model we draw for the $\gamma\gamma PS$ and $\gamma\mathbb{O}PS$ form factors $T^{\gamma\gamma}$ [$\equiv T$ of (10)] and $T^{\gamma\mathbb{O}}$ the diagrams shown in Fig. 4. Assuming all *PS*-wave function effects to be identical in the diagrams (a) and (b) of Fig. 4, and denoting by Q_i the quark charge in units of the proton charge, we get

$$\frac{T^{\gamma\mathbb{O}}}{T^{\gamma\gamma}}=\frac{e\beta_{\mathbb{O}}\sum_i a_{PS}^i Q_i}{e^2\sum_i a_{PS}^i Q_i^2}\equiv\frac{\beta_{\mathbb{O}}}{e}\,r_{PS}. \quad (49)$$

Within this valence quark model, the relative coupling strengths may then be derived by assuming that the pion is an isospin triplet, the η and η' are mixtures of $SU(3)$ singlet and octet with mixing angle θ, and the η_c is a pure $c\bar{c}$ state:

$$r_\pi=3\,,\qquad r_\eta=3\cos\theta\,,$$
$$r_{\eta'}=-3\sin\theta\,,\qquad r_{\eta_c}=3/2\,. \quad (50)$$

Since a $SU(3)$ singlet decouples, in the limit $\theta=0$ the odderon coupling of the η' vanishes. In the following analysis we will take the value $\theta=-20^\circ$ [11].

With these assumptions, the amplitude for the sum of the diagrams Fig. 1a,b is obtained from the $\gamma\gamma$-amplitude by a simple replacement for the term corresponding to the propagator of the photon $\gamma(q_2)$:

$$\frac{e^2}{t_2}\longrightarrow\frac{e^2}{t_2}+3r_{PS}\,\eta_{\mathbb{O}}\,\beta_{\mathbb{O}}^2\left(-i\frac{s_2}{s_0}\right)^{\alpha_{\mathbb{O}}(t_2)-1} \quad (51)$$

Our ansatz depends on the quark-odderon coupling $\beta_{\mathbb{O}}$, on the phase $\eta_{\mathbb{O}}$, and on the three parameters $\alpha_{\mathbb{O}}(0),\alpha'_{\mathbb{O}},s_0$. As reference values we choose

$$\alpha_{\mathbb{O}}(0)=1\,,\qquad \alpha'_{\mathbb{O}}=0.25\text{ GeV}^{-2}\,,\qquad s_0=1\text{ GeV}^2\,,$$
$$\eta_{\mathbb{O}}=-1\,,\qquad \beta_{\mathbb{O}}^2=0.05\,\beta_{\mathbb{P}}^2\,, \quad (52)$$

where $\beta_{\mathbb{P}}=1.8$ GeV^{-1} is the quark-pomeron coupling. The abbreviation

$$c_{\mathbb{O}}=\eta_{\mathbb{O}}\,\beta_{\mathbb{O}}^2/\beta_{\mathbb{P}}^2 \quad (53)$$

turns out to be convenient for the presentation of our numerical results below.

By comparing the measured total cross sections in different channels with the expectation from photon-photon fusion alone, the odderon couplings can in principle be determined and the model values (50) be tested. In Fig. 5 we display the values of the cross section in the photoproduction region as a function of the odderon coupling parameter $c_{\mathbb{O}}$. Clearly, the effect of the odderon on η' production is much weaker than on π^0 or η production. However, due to the experimental uncertainty in the value of $\Gamma_{\gamma\gamma}$ (cf. Table 1), the normalization of the photon-photon cross section is known only to 10% accuracy. Hence, in order to be sensitive to the odderon coupling strength, it is important to separate its contribution kinematically, as we will discuss in the following section.

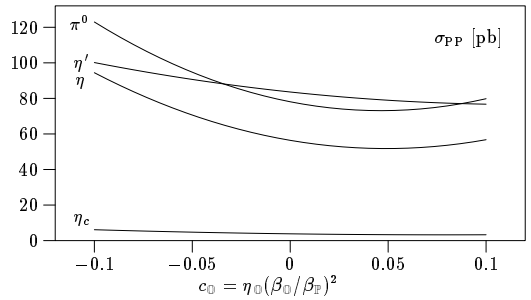

Fig. 5. Total cross section for pseudoscalar meson production in the photoproduction region (8) as a function of the odderon coupling $c_{\mathbb{O}}$. The other parameters are taken at their reference values (52), and the relative coupling strengths are taken from (50)

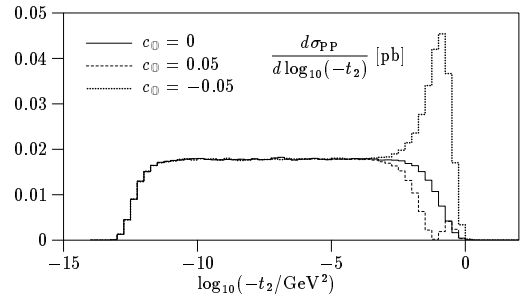

Fig. 6. t_2 distribution for pion production in the PP region (8)

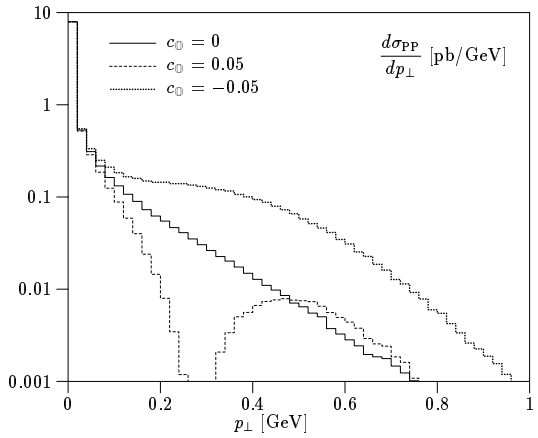

Fig. 7. $p_\perp$ distribution for pion production in the PP region (8)

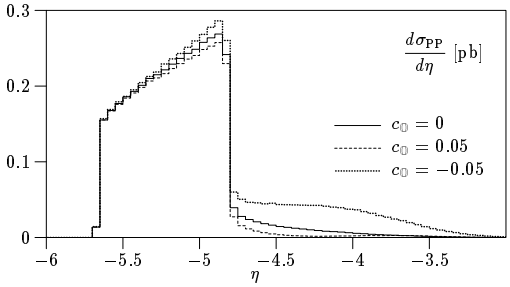

Fig. 8. Rapidity distribution for pion production in the PP region (8)

5 Phenomenology

The most characteristic feature of the hadronic interaction in Fig. 1b is the absence of the propagator pole in t_2. In this respect, the hadronic vertex behaves similar to a four-particle contact term. Its presence should therefore manifest itself by an enhancement (or a reduction) of events with large values of t_2 due to a constructive (destructive) interference of the two diagrams in Fig. 1. This is illustrated in Fig. 6, where we show the differential cross section with respect to the logarithm of t_2 for the PP cuts (8). Whereas photon exchange results in a distribution in $\log|t_2|$ which is constant over many decades, the hadronic contribution is concentrated in the region between 0.01 and 1 GeV^2. Depending on the sign $\eta_{\mathbb{O}}$ of the odderon coupling, there is positive or negative interference with the photon-photon fusion amplitude.

In diffractive scattering t_2 is usually not easily observable. However, in the photoproduction region where $Q^2 \approx 0$, the transverse momentum squared $p_\perp^2$ of the final-state meson is approximately equal to $-t_2$. Thus, for negative sign, $\eta_{\mathbb{O}} = -1$, the odderon contribution shows up as an enhancement of the higher $p_\perp$ values (cf. Fig. 7). If $\eta_{\mathbb{O}}$ is positive, the odderon amplitude is of opposite sign to the photon-photon amplitude. This effect results in a dip in the $p_\perp$ distribution at the value where the interference is maximal.

The hadronic contribution is visible also in other observables: For instance, if the PP cuts are applied, the rapidity η of the final-state meson is bounded [cf. (31)]

$$\eta \le \eta_{\rm cm} - \log\frac{\sqrt{s}}{m_{PS}} - \log y_{\rm min} \tag{54}$$

if t_2 can be neglected, which holds true for the bulk of the photon-photon cross section, but not for the odderon contribution. Thus, the odderon affects the tail in the rapidity distribution (Fig. 8), and a cut on η near $\eta_{\rm max}$ is one possibility for separating the odderon contribution. A similar consideration applies to the invariant mass s_1 of the electron-meson system.

These signatures are essentially independent of the particular parameterization (51) we chose for the hadronic vertex. A more specific test of the odderon hypothesis would be to measure the parameters the ansatz (51) depends on.

Regge phenomenology predicts a power dependence on the hadronic subenergy:

$$\frac{d\sigma}{dt_2}(t_2 = 0) \propto (s_2/s_0)^{\alpha_{\mathbb{O}}(0)-1}. \tag{55}$$

For the pomeron, a value of $\alpha_{\mathbb{P}}(0) > 1$ has been observed [10]. This behavior may also occurr for the odderon; in addition, there are subleading contributions [*e.g.*, an ω trajectory with $\alpha_\omega(0) \sim 0.5$]. Compared to photon exchange, the hadronic contribution becomes dominant at asymptotic energies if $\alpha_{\mathbb{O}}(0) > 1$, or "dies out" in the opposite case. In order to be sensitive to the exponent $\alpha_{\mathbb{O}}(0)$,

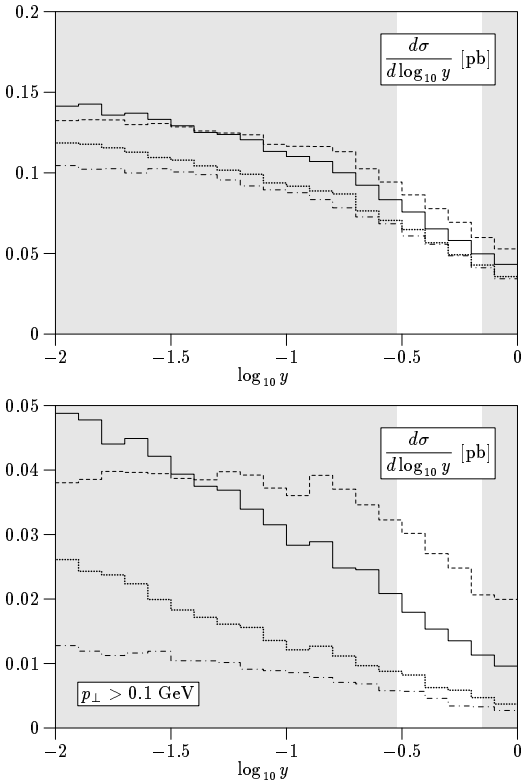

Fig. 9. *Upper part*: $\log y$ distribution for pion production in the PP region. *Solid line*: $\alpha_{\mathbb{O}}(0) = 1$, $c_{\mathbb{O}} = -0.05$; *dashed*: $\alpha_{\mathbb{O}}(0) = 1.2$, $c_{\mathbb{O}} = -0.01$; *dotted*: $\alpha_{\mathbb{O}}(0) = 0.8$, $c_{\mathbb{O}} = -0.10$. The other parameters are as given in (52). The *lowest curve* (*dash-dots*) corresponds to photon-photon fusion alone ($c_{\mathbb{O}} = 0$). *Lower part*: The analogous distributions with a cut $p_\perp > 0.1$ GeV for the produced meson applied. The window in y selected by the cuts (8) is indicated by the *unshaded band*

the hadronic subenergy $\sqrt{s_2} = W$, or, equivalently, the electron energy loss y, should be measured over several decades. In Fig. 9 we display the distribution in y for pion photoproduction for the values $\alpha_{\mathbb{O}}(0) = 0.8$, 1, and 1.2. The odderon coupling has been adjusted in each case such that the total PP cross sections are comparable. Without additional cuts, a difference in the slope of the y distributions is hardly detectable. If, on the other hand, a $p_\perp$ cut of 0.1 GeV for the produced pion is applied, the $\gamma\gamma$ background is reduced and the shape of the three curves can easily be distinguished. However, in order to disentangle the measurements of $\alpha_{\mathbb{O}}(0)$ and of the odderon coupling $\beta_{\mathbb{O}}$ by this method, it is necessary that y values down to 10^{-2} are accessible, or, equivalently, experiments are carried out at lower collider energies.

At HERA, for low values of Q^2 the hadronic subenergy is given by $W \sim \sqrt{ys} = 300\ \text{GeV} \times \sqrt{y}$. Thus, non-leading Regge terms as discussed above should be very small for $0.03 \lesssim y \leq 1$, corresponding to 50 GeV $\lesssim W \lesssim$ 300 GeV. For smaller y and/or c.m. energies such non-leading terms should be included in the analysis.

With sufficient statistics, the dependence on t_2 can be determined from the meson's $p_\perp$ distribution, and the odderon form factors can be measured. In Fig. 10 we show

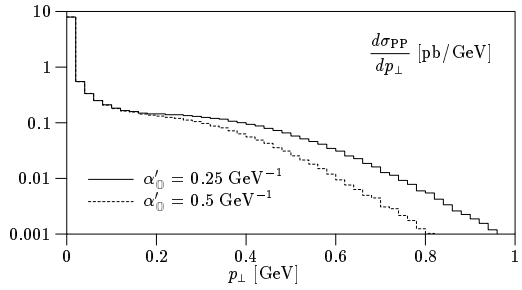

Fig. 10. $p_\perp$ distribution for pion production in the PP region (8). The odderon coupling is fixed to $c_{\mathbb{O}} = -0.05$

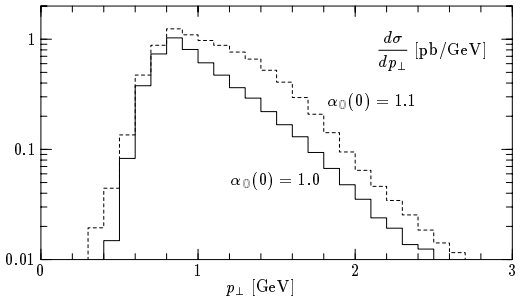

Fig. 11. $p_\perp$ distribution for π^0 production in the DIS region (9). The two curves correspond to two different values of the exponent $\alpha_{\mathbb{O}}$. The other parameters are fixed to their reference values (52)

the influence of the value of the parameter $\alpha'_{\mathbb{O}}$ which controls the exponential falloff of the odderon amplitude, Changing $\alpha'_{\mathbb{O}}$ from 0.25 GeV^{-1} to 0.5 GeV^{-1}, results in a reduction of events with $p_\perp > 0.2$ GeV if the phase of the odderon coupling is negative. In the opposite case ($\eta_{\mathbb{O}} = +1$), this change shifts the position of the dip in the $p_\perp$ distribution, the experimental observation of which, however, requires high event rates.

6 Transition to the hard region

In vector meson production at HERA, deviations from the universal "soft pomeron" behavior are observed whenever there is a hard scale which limits the effective transverse size of the interaction region [41]. In particular, if either the initial photon has a high virtuality or the produced meson has a large mass (*e.g.*, $J/\psi, \Upsilon$) in comparison to the typical hadronic scale ~ 1 GeV, the dependence on s becomes steeper.

A similar transition to the hard region should also be observable in the processes considered in this paper. As illustrated in Fig. 11, in the DIS region the effect of an increase in the exponent $\alpha_{\mathbb{O}}(0)$ shows up as a broadening of the $p_\perp$ distribution, since an enhancement of the odderon contribution with respect to the $\gamma\gamma$ amplitude allows for higher values of the momentum transfer t_2. If the $p_\perp$ distribution in the DIS region is compared to the corresponding distribution in photoproduction, it is possible in principle to isolate the effect of a hard scale in the interaction. Furthermore, the transition form factor of the η_c

meson is expected to decrease more slowly than the form factors of the light mesons [34]. For this reason, the production cross section for the η_c meson in the DIS region is of comparable size to the cross section of light pseudoscalar mesons (cf. Table 2), and the observed η_c production rate can serve as another probe of a possible hard odderon[2], if total cross sections of magnitude 1 pb or less are within the experimental reach. [Note that an increase of the accessible y range would enhance the observable rates considerably, similar to the photoproduction case as illustrated in Fig. 9.]

7 Conclusions

In this article we have discussed in detail exclusive pseudoscalar meson production in $e^{\pm}p$ scattering at HERA energies. For the contribution from $\gamma\gamma$-fusion we gave numerical values obtained from two versions of the equivalent photon approximation: (i) applied to both the photon from the electron line and the proton line (DEPA) and (ii) applied to the photon from the electron line only (EPA). The full calculation showed that DEPA (EPA) give accuracies of order 20% ($< 5\%$) for total cross sections without cuts and with photoproduction cuts (8). For the deep-inelastic scattering cuts (9) only the full calculation is reliable[3].

In Sect. 4 we introduced a simple ansatz for a possible odderon exchange contribution to exclusive pseudoscalar meson production. We showed how this odderon affects total cross sections and differential distributions. Interference effects are large in the parameter region of interest and have been taken into account. Particularly promising as signals for the odderon are the t_2 and $p_\perp$ distributions (Figs. 6–7). A larger acceptance in the variable y (7) than assumed in (8,9) would increase the cross sections considerably (Fig. 9). This would lead to a greatly increased potential for finding the odderon and determining its parameters.

In the HERA kinematical situation, events with $Q^2 \lesssim 10\ \mathrm{GeV}^2$ and $0.03 \lesssim y \leq 1$ correspond to a hadronic energy W between 50 and 300 GeV. This should be large enough for non-leading Regge terms to be suppressed. However, it is straightforward to include such terms in the theoretical formulae for a detailed analysis of experimental data.

The cross sections we have calculated for pseudoscalar meson production at HERA are between 0.5 and 1800 pb, depending on the produced meson and on the particular cuts imposed (cf. Table 2 and Fig. 5). With an integrated luminosity of 30 pb^{-1} per year such processes should definitely be observable and give valuable insight in the mechanisms of diffraction in QCD.

[2] A perturbative estimate for η_c production via odderon exchange can be found in [42]

[3] The Monte Carlo programs used for the calculations are available from the authors

Acknowledgements. We are grateful to T. Berndt, H.-G. Dosch, P.V. Landshoff, K. Meier, T. Ohl, M. Rüter, R. Ruskov, and S. Tapprogge for fruitful discussions and valuable comments. We also thank H.-G. Dosch and P.V. Landshoff for a critical reading of the manuscript.

References

1. F.E. Low, Phys. Rev. **D12** (1975) 163; S. Nussinov, Phys. Rev. Lett. **34** (1975) 1286
2. H. Cheng, T.T. Wu, Expanding Protons, MIT Press, Cambridge, Mass. (1987) and references therein
3. J.F. Gunion, D.E. Soper, Phys. Rev. **D15** (1977) 2617
4. E.A. Kuraev, L.N. Lipatov, V.S. Fadin, Sov. Phys. JETP **44** (1976) 443; L.N. Lipatov, Sov. J. Nucl. Phys. **23** (1976) 338; Y.Y. Balitskij, L.N. Lipatov, ibid. **28** (1978) 822
5. P.V. Landshoff, O. Nachtmann, Z. Phys. **C35** (1987) 405
6. O. Nachtmann, Ann. Phys. (N.Y.) **209** (1991) 436
7. H.G. Dosch, E. Ferreira, A. Krämer, Phys. Rev. **D50** (1994) 1992
8. O. Nachtmann, High Energy Collisions and Nonperturbative QCD, in: Perturbative and Nonperturbative Aspects of Quantum Field Theory, H. Latal, W. Schweiger (eds.), Springer Verlag (1997)
9. P.D.B. Collins, An Introduction to Regge Theory, Cambridge University Press (1977); L. Caneschi (ed.), Regge Theory of low p_T hadronic interaction, North Holland, Amsterdam (1989)
10. A. Donnachie and P.V. Landshoff, Nucl. Phys. **B244** (1984) 322; ibid. **B267** (1986) 690; Phys. Lett. **B185** (1987) 403
11. R.M. Barnett et al. (Particle Data Group), Phys. Rev. **D54** (1996) 1
12. L. Van Hove, Phys. Let. **B24** (1967) 183
13. C.J. Morningstar, M. Peardon, Phys. Rev. **D56** (1997) 4043; M. Teper, Preprint OUTP–97–66P, hep-ph/9711299, to appear in: Proceedings of the Europhysics HEP Conference, Jerusalem, August 1997
14. P.V. Landshoff, The two pomerons, in: Proceedings of the Summer School on Hadronic Aspects of Collider Physics, Zuoz, 1994, M.P. Locher (ed.), PSI, Villigen (1994)
15. L.N. Lipatov, Pomeron in Quantum Chromodynamics, in: Perturbative Quantum Chromodynamics, A.H. Mueller (ed.), World Scientific, Singapore (1989)
16. J.R. Forshaw, D.A. Ross, Quantum chromodynamics and the pomeron, Cambridge University Press (1997)
17. L. Lukaszuk, B, Nicolescu, Nuov. Cim. Lett. **8** (1973) 405; D. Joynson, E. Leader, C. Lopez, B. Nicolescu, Nuov. Cim. **30A** (1975) 345
18. D. Bernard, P. Gauron, B. Nicolescu, Phys. Lett. **B199** (1987) 125; P. Gauron, E. Leader, B. Nicolescu, Phys. Rev. Lett. **54** (1985) 2656; ibid. **55** (1985) 639
19. E. Leader, Phys. Lett. **B253** (1991) 457
20. R.J.M. Corolan, P. Desgrolard, M. Giffon, L.L. Jenkovszky, E. Predazzi, Z. Phys. **C58** (1993) 109
21. L.N. Lipatov, Preprint DESY 90–060 (unpublished); P. Gauron, L. Lipatov, B. Nicolescu, Phys. Lett. **B304** (1993) 334
22. N. Armesto, M.A. Braun, Preprint DESY-97-150, hep-ph/9708296
23. B.V. Struminskii, Phys. Atom. Nucl. **57** (1994) 1398

24. G.P. Korchemsky, Nucl. Phys. **B462** (1996) 333; R.A. Janik, J. Wosiek, Phys. Rev. Lett. **79** (1997) 2935
25. A. Donnachie, P.V. Landshoff, Nucl. Phys. **B348** (1991) 297
26. I.F. Ginzburg, JETP Lett. **59** (1994) 605
27. H.G. Dosch, M. Rueter, Phys. Lett. **B380** (1996) 177
28. A. Schäfer, L. Mankiewicz, O. Nachtmann, in: Proceedings of the 1991 DESY/HERA Workshop (W. Buchmüller, G. Ingelman, eds.)
29. S. Tapprogge, Ph.D. Thesis, Report HD–IHEP 96–19, and private communication
30. S.J. Brodsky, G.P. Lepage, Phys. Rev. **D24** (1981) 1808
31. V.V. Anisovich, D.I. Melikhov, V.A. Nikonov, Phys. Rev. **D55** (1997) 2918
32. A.V. Radyushkin, R. Ruskov, Phys. Lett. **B374** (1996) 173; Nucl. Phys. **B481** (1996) 625
33. H.-J. Behrend et al. (CELLO Collaboration), Z. Phys. **C49** (1991) 401; H. Aihara et al. (TPC/2γ Collaboration), Phys. Rev. Lett. **64** (1990) 172; V. Savinov (CLEO Collaboration), in: Proceedings of the 10th Workshop on Photon-Photon Collisions (PHOTON '95), Sheffield, England, April 8-13 1995
34. T. Feldmann, P. Kroll, Phys. Lett. **B413** (1997) 410
35. G. Köpp, T.F. Walsh, P.M. Zerwas, Nucl. Phys. **B70** (1974) 461; S.J. Brodsky, G.P. Lepage, Phys. Rev. **D22** (1980) 2157
36. V.M. Budnev, I.F. Ginzburg, G.V. Meledin, V.G. Serbo, Phys. Rep. **15** (1975) 181
37. F. Borkowski et al., Nucl. Phys. **B93** (1975) 461; P.E. Bosted et al., Phys. Rev. Lett. **68** (1992) 3841
38. E.E. Boos, M.N. Dubinin, V.A. Ilyin, A.E. Pukhov, V.I. Savrin, Report SNUTP–94–116, hep-ph/9503280 (unpublished); P.A.Baikov et al., in: Proceedings of the Workshop QFTHEP-96, eds. B. Levtchenko, V. Savrin, (Moscow 1996), hep-ph/9701412
39. G. Schuler, Preprint CERN–TH 96/313, hep-ph/9611249; Preprint CERN–TH 97/265, hep-ph/9710506
40. C. Augier et al. (UA 4/2 Collab.), Phys. Lett. **B316** (1993) 448; N.A. Amos et al. (E–710 Collab.), Phys. Rev. Lett. **68** (1992) 2433
41. E. Gallo, to appear in: Proceedings of the XVIII International Symposium on Lepton-Photon interactions, Hamburg, July 1997
42. J. Czyżewski, J. Kwieciński, L. Motyka, M. Sazikowski, Phys. Lett. **B398** (1997) 400, (E) ibid. **B411** (1997) 402; R. Engel, D.Y. Ivanov, R. Kirschner, L. Szymanowski, Preprint DESY-97-139, hep-ph/9707362